Advances in Radiation Oncology (2024) 9, 101336

advances in radiation oncology

www.advancesradonc.org

Scientific Article

A Technique to Enable Efficient Adaptive Radiation Therapy: Automated Contouring of Prostate and Adjacent Organs

Daniel E. Hyer, PhD,[a,*] Joseph Caster, MD, PhD,[a] Blake Smith, PhD,[a] Joel St-Aubin, PhD,[a] Jeffrey Snyder, MS,[a] Andrew Shepard, PhD,[a] Honghai Zhang, PhD,[b] Sean Mullan, MS,[b] Theodore Geoghegan, MS,[a] Benjamin George, BA,[a] James Byrne, MD, PhD,[a] Mark Smith, MD,[a] John M. Buatti, MD,[a] and Milan Sonka, PhD[b]

[a]*Department of Radiation Oncology, University of Iowa Hospitals and Clinics, Iowa City, Iowa; and* [b]*Iowa Institute for Biomedical Imaging, University of Iowa, Iowa City, Iowa*

Received 19 December 2022; accepted 31 July 2023

Purpose: The purpose of this work was to investigate the use of a segmentation approach that could potentially improve the speed and reproducibility of contouring during magnetic resonance–guided adaptive radiation therapy.

Methods and Materials: The segmentation algorithm was based on a hybrid deep neural network and graph optimization approach that also allows rapid user intervention (Deep layered optimal graph image segmentation of multiple objects and surfaces [LOGISMOS] + just enough interaction [JEI]). A total of 115 magnetic resonance–data sets were used for training and quantitative assessment. Expert segmentations were used as the independent standard for the prostate, seminal vesicles, bladder, rectum, and femoral heads for all 115 data sets. In addition, 3 independent radiation oncologists contoured the prostate, seminal vesicles, and rectum for a subset of patients such that the interobserver variability could be quantified. Consensus contours were then generated from these independent contours using a simultaneous truth and performance level estimation approach, and the deviation of Deep LOGISMOS + JEI contours to the consensus contours was evaluated and compared with the interobserver variability.

Results: The absolute accuracy of Deep LOGISMOS + JEI generated contours was evaluated using median absolute surface-to-surface distance which ranged from a minimum of 0.20 mm for the bladder to a maximum of 0.93 mm for the prostate compared with the independent standard across all data sets. The median relative surface-to-surface distance was less than 0.17 mm for all organs, indicating that the Deep LOGISMOS + JEI algorithm did not exhibit a systematic under- or oversegmentation. Interobserver variability testing yielded a mean absolute surface-to-surface distance of 0.93, 1.04, and 0.81 mm for the prostate, seminal vesicles, and rectum, respectively. In comparison, the deviation of Deep LOGISMOS + JEI from consensus simultaneous truth and performance level estimation contours was 0.57, 0.64, and 0.55 mm for the same organs. On average, the Deep LOGISMOS algorithm took less than 26 seconds for contour segmentation.

Conclusions: Deep LOGISMOS + JEI segmentation efficiently generated clinically acceptable prostate and normal tissue contours, potentially limiting the need for time intensive manual contouring with each fraction.

Sources of support: This work was supported in part by National Institutes of Health grants R01-EB004640 and T32-HL144461.
Research data are not available at this time.

*Corresponding author: Daniel E. Hyer, PhD; email: daniel-hyer@uiowa.edu

https://doi.org/10.1016/j.adro.2023.101336

Introduction

Daily delineation of the intended target and nearby critical structures is a critical step for magnetic resonance imaging (MRI)−guided adaptive radiation therapy (MRIgART). During the inverse planning process, dosimetric objectives placed on these structures define the shape of the final dose distribution, and the bulk density assignments of each structure are commonly used for dose calculations on the MRI. When an online plan adaption is necessary, contemporary MRIgART workflows include a deformation of the reference plan contours, which frequently includes the time-consuming step of manual editing followed by reoptimization of the treatment plan. An average MRIgART treatment session time ranges between 53 to 80 minutes,[1-4] depending on the site and complexity of the plan. The contour delineation constitutes a significant portion of this time, ranging between 10 to more than 20 minutes.[1,5]

Specific to prostate cancer, both deep-learning and atlas-based algorithms have been published to facilitate improved autosegmentation of the prostate and other low-contrast organs.[6-8] Although these algorithms may enable rapid autosegmentation, they still required manual editing to make any corrections when the contours need adjustment. To overcome these challenges, this work implements a segmentation tool called deep layered optimal graph image segmentation of multiple objects and surfaces (LOGISMOS) + just enough interaction (JEI),[9] which is based on a hybrid deep neural network and graph optimization approach, for use in MRIgART. An early application of the LOGISMOS segmentation approach for prostate delineation was reported by Yin et al,[10] with promising results for segmenting the prostate's central gland and its peripheral zone. However, this early application required manual selection of the volume of interest and lacked any means to efficiently adjudicate the resulting segmentation surfaces when needed. In addition, no segmentation of additional nearby organs at risk was performed. The approach reported here builds on our earlier work by newly introducing a deep learning presegmentation to guide the LOGISMOS segmentation for the prostate and surrounding organs at risk. In addition, and only when needed, the proposed technique integrates physician guidance through a JEI approach to streamline the editing of automated contours.[8] To the best of our knowledge, no similar approach has been proposed for MRIgART that allows for automated yet quickly editable contours on the fly. We expect this approach to not only result in efficiency improvements, but also improve the reproducibility with respect to manually drawn contours, which is particularly important for standardization of radiation therapy and the accuracy of outcomes measured from clinical trials.

Methods and Materials

Deep LOGISMOS + JEI

The LOGISMOS approach and its most recent Deep LOGISMOS incarnation have been developed by this team—much of the infrastructure is a result of multiple phases of National Institutes of Health/National Institute of Biomedical Imaging and Bioengineering research project R01-EB004640. At its core, Deep LOGISMOS, as illustrated in Fig. 1, is an automated *n*-dimensional image segmentation approach that uses a novel combination of deep learning and optimal graph-based identification of multiple mutually interacting

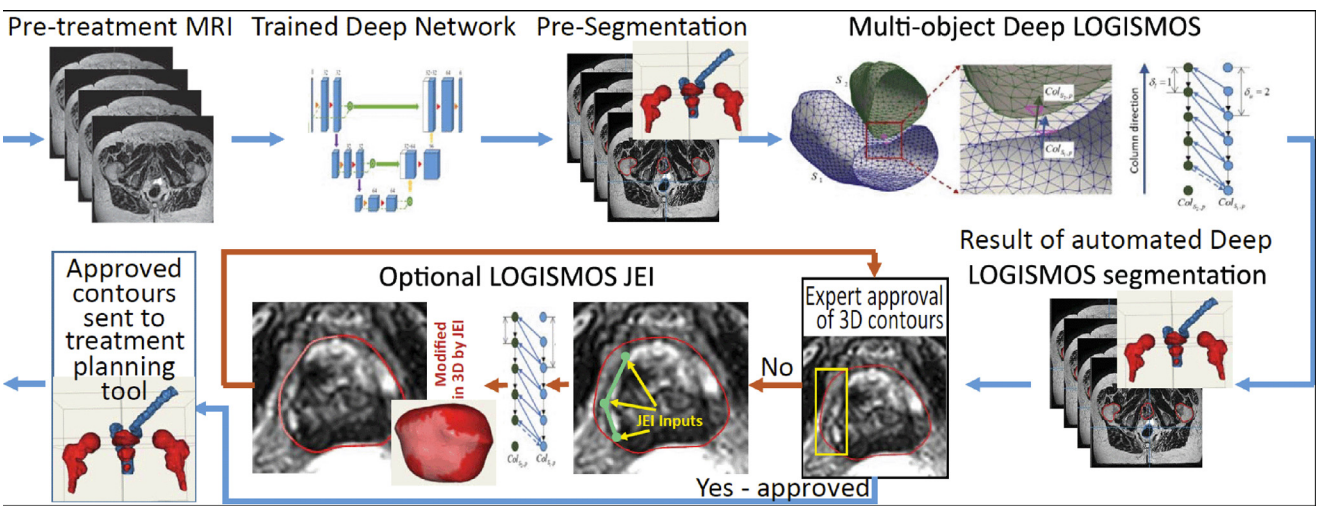

Figure 1 Schematic of the automated Deep LOGISMOS + JEI for adaptive prostate radiation therapy planning with expert-guidance option. *Abbreviation:* JEI = just enough interaction; LOGISMOS = layered optimal graph image segmentation of multiple objects and surfaces; MRI, magnetic resonance imaging.

objects and their surfaces.[11] With Deep LOGISMOS, the process is initiated by a deep-learning preliminary segmentation followed by graph-based optimization, guaranteeing topological consistency and global optimality with respect to a task-specific machine-learned cost function. The LOGISMOS approach uses a set of surface- and/or region-specific costs, representing the multisurface segmentation task as a graph optimization problem, and finds the optimal solution via $s-t$ cut graph optimization.[12-15] As a result, all target objects and their surfaces are segmented simultaneously in 3-dimensions (3D) in a single optimization process that employs not only information about the surface properties but also uses regional information about image appearance of the individual objects and anatomy-based information about mutual object-to-object interactions.[11,13,16-19] If clinically necessary, the automated Deep LOGISMOS result can be augmented by JEI, an additional step of expert guidance. This approach affects the underlying graph-optimization algorithm to achieve clinically appropriate 3D segmentations of organs/objects of interest and facilitate subsequent treatment planning steps. For this application, Deep LOGISMOS + JEI was designed to universally and consistently obtain the desired segmentation of the prostate and surrounding tissues (seminal vesicles, bladder, rectum, and left/right femur heads) required for radiation treatment planning.

Deep-learning presegmentation

The deep-learning presegmentation module is based on the "convolutional neural network and a transformer" architecture developed by Xie et al,[20] as it learns long-range dependencies from features extracted by a convolutional neural network from the input images. We selected this specific architecture as its multiscale deformable self-attention mechanism enables us to leverage the representational power of a transformer network across multiple scales of encoded features while still having the computational efficiency to process large input regions that better leverage the relationships between different anatomic landmarks in 3D. Our network operates on input patches with a size of $160 \times 160 \times 96$ voxels and outputs separate predicted segmentation maps for each of the desired structures and the background. During inference, these volume patches are evaluated across the entire target volume.

To facilitate the training of our model, we used the nnU-Net training pipeline.[21] During preprocessing, all training volumes were resampled to $0.83 \times 0.83 \times 1.00$ mm spacing, and intensity values were standardized to 0 mean and unit variance for each volume separately. To mitigate the risk of overfitting on our limited data set, we applied random data augmentations to all training samples. Random augmentations included up to a 15° rotation along each axis, resizing along each axis within a range of 85% to 125% of image size, mirroring operations along each axis, and gamma adjustment within the range of 0.7 to 1.5, with the augmentations and augmentation intensities selected independently for each training sample. The training process was performed over 1000 epochs with a polynomial decay learning rate schedule. The learning rate was initialized with a value of 0.01 and updated at the end of each epoch with the policy: $0.01 \times (1 - \text{epoch}_{\text{current}} / \text{epoch}_{\text{max}})^{0.9}$. For each training sample, loss was computed using combined generalized Dice and cross entropy terms with equal weights for each term. Only 2 samples were used in each batch, and instance normalization was used rather than the more standard batch normalization for our model layers.

Multi-object segmentation of prostate and surrounding organs

The presegmentation results were converted to triangular mesh surfaces using a standard marching cube algorithm and then smoothed and decimated (number of triangles reduced). LOGISMOS graphs, 1 for each organ, were constructed based on the resulting surface meshes such that each vertex of the mesh is associated with a column that goes from the inside of the mesh to the outside along the surface normal direction (Fig. 1). The typical (adjustable if needed) length of the graph column was 5 mm for the seminal vesicles and 10 mm for the other organs, with the mesh surface passing through the middle of the columns, determined experimentally to reflect the observed distances between the presegmentation and desired organ surfaces in the training set. The spacing between graph nodes on a column was 0.4 mm. Edge-based cost functions were used. Following automated Deep LOGISMOS segmentation, an expert user visually inspects the results and has the option to correct potential inaccuracies (Fig. 1). Finally, the segmentations are converted back to labeled volumes for quantitative analysis.

Training and evaluation

To demonstrate the feasibility of Deep LOGISMOS + JEI for adaptive prostate cancer radiation treatment, 115 daily MR data sets acquired pretreatment for adaptive therapy (T2 weighted, 2-minute acquisition; Elekta Unity) from 23 unique patients were used to evaluate the performance of the pilot Deep LOGISMOS + JEI implementation for prostate cancer treatments. Each data set was manually contoured by a clinical expert for the prostate, bladder, seminal vesicles, rectum, and left and right femur heads. Training and quantitative testing were performed using a 5-fold, leave 20% out cross-validation technique. The training folds were stratified by subject to ensure no model was evaluated on data sets acquired from subjects represented in the training data.

Quantitative assessment of the predicted contours was performed using absolute surface-to-surface distance (ASSD),

relative surface-to-surface distance (RSSD), the 95th percentile Hausdorff distance, and the Dice similarity coefficient (DSC). ASSD was calculated by computing the shortest distance from each point on the predicted contour surface to a point on the independent standard surface and taking the average across all such distances for the given contour. RSSD was calculated using the same method, but distances where the predicted contour surface is located within (inside of) the independent standard contour surface are considered negative. The maximum Hausdorff distance is the maximum distance from a point on either contour surface to the closest point on the other. As the maximum can be heavily skewed by even a single outlier, we instead measured the 95th percentile Hausdorff distance by computing the 95th percentile of these distances rather than the maximum. Lastly, the DSC is a measure of volumetric overlap that was evaluated by computing twice the volume of the considered contours' intersection divided by the sum of the individual volumes of the 2 contours.

To assess whether the achieved processing times were sufficiently short for clinical use in adaptive radiation treatment planning, computational times of the automated Deep LOGISMOS, times needed for inspection and optional JEI, and combined processing times were measured for each analyzed case.

To demonstrate the reproducibility improvements resulting from Deep LOGISMOS + JEI compared with interobserver variability of expert manual tracings, 3 radiation oncologists that specialize in the treatment of prostate cancer manually contoured the prostate, seminal vesicles, and rectum in 3 patients with body mass indices of 21, 25, and 32, respectively. Consensus contours were created using the simultaneous truth and performance level estimation (STAPLE) approach,[22] and interobserver variabilities of manual contours and the deviation of Deep LOGISMOS + JEI contours from the consensus contours was calculated. Contours were evaluated using the same quantitative metrics described previously.

Results

Results of the validation of the Deep LOGISMOS + JEI method performed against the 115 expert-contoured data sets is shown in Fig. 2. The absolute accuracy of Deep LOGISMOS + JEI generated contours was evaluated using median ASSD, which ranged from a minimum of 0.20 mm for the bladder to a maximum of 0.93 mm for the prostate compared with the independent standard

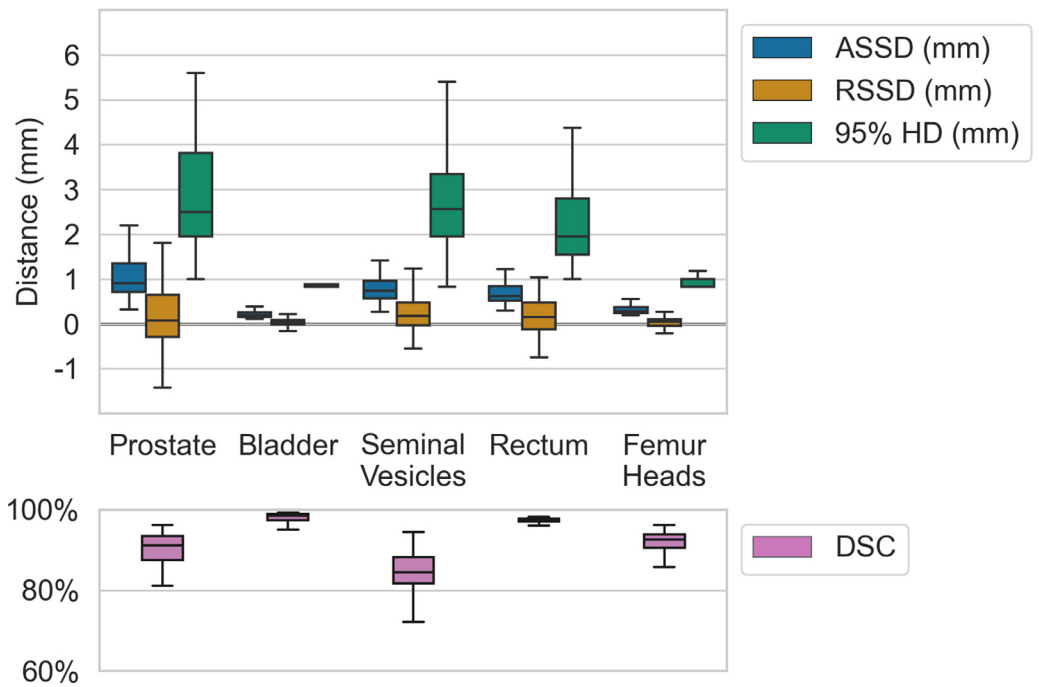

Figure 2 Quantitative assessment of segmentation performance achieved by Deep LOGISMOS + just enough interaction in prostate and 5 surrounding organs using 5-fold cross-validation in 115 daily magnetic resonance data sets. DSC, ASSD, RSSD, and 95% HD, plotted as boxplots with 1.5 interquartile range whiskers, demonstrate that 3-dimensional segmentation performance is consistently within millimeters of the manually defined independent standard. Note the close-to-zero RSSD values demonstrating minimal bias of the Deep LOGISMOS + just enough interaction approach (no consistent under- or oversegmentation). *Abbreviation:* ASSD = absolute surface-to-surface distance; DSC = dice similarity coefficient; HD = Hausdorff distance; LOGISMOS = layered optimal graph image segmentation of multiple objects and surfaces; RSSD = relative surface-to-surface distance.

across all data sets. The median RSSD was less than 0.17 mm for all organs, indicating that the Deep LOGISMOS + JEI algorithm did not exhibit a systematic under- or oversegmentation. The median DSC value was more than 91.2% across all organs excluding the seminal vesicles, indicating a high degree of shape similarity between the Deep LOGISMOS + JEI and expert contours. The seminal vesicles had a DSC of 84.2%. The median 95% Hausdorff distance was less than 2.6 mm, indicating limited outliers in surface consistency.

Application of the Deep LOGISMOS algorithm on the daily prostate MR data sets took 25.8 ± 0.2 seconds on average for the 3D 6-organ segmentation. Expert review and optional JEI took an additional 2 to 3 minutes in cases for which interactive editing was needed. This represents a significant time reduction compared with an average of 14 minutes for completely manual edits on a slice-by-slice basis, which is the current standard.[1]

One major advantage of the Deep LOGISMOS + JEI method is the potential to improve reproducibility compared with interobserver variability of expert manual tracings. Figure 3 visually compares a single-user LOGISMOS + JEI result with consensus STAPLE contours for patients of variable size. Detailed metrics are summarized in Fig. 4, where the interobserver variability between the 3 expert contours used to create the

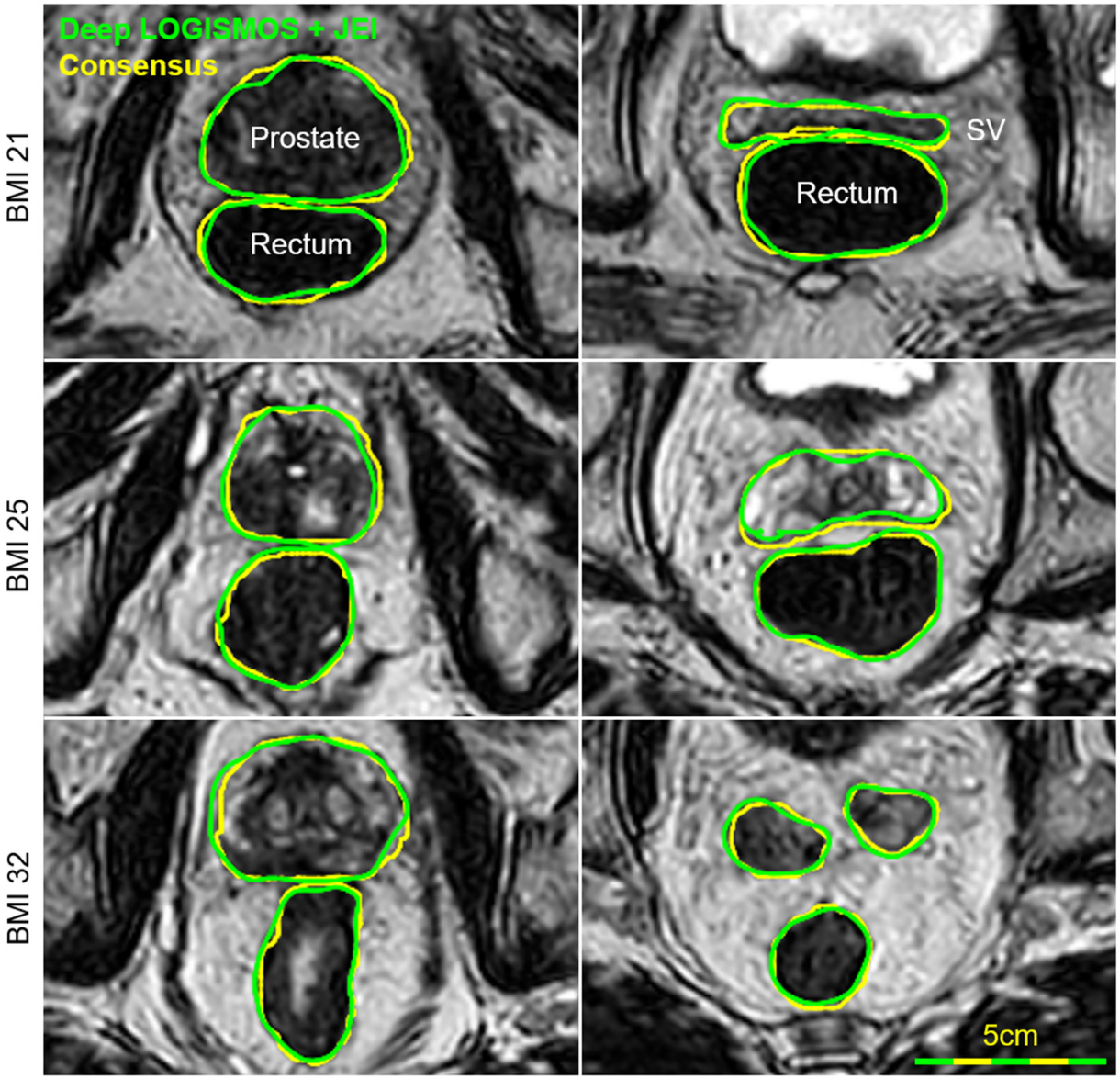

Figure 3 Deep LOGISMOS + JEI; (green) versus consensus contours (yellow) for 3 patients of variable BMI. Two axial slices are shown for each patient to visualize the interfaces between both the prostate/rectum and the SV/rectum. *Abbreviations:* BMI = body mass index; JEI = just enough interaction; LOGISMOS = layered optimal graph image segmentation of multiple objects and surfaces; SV = seminal vesicles.

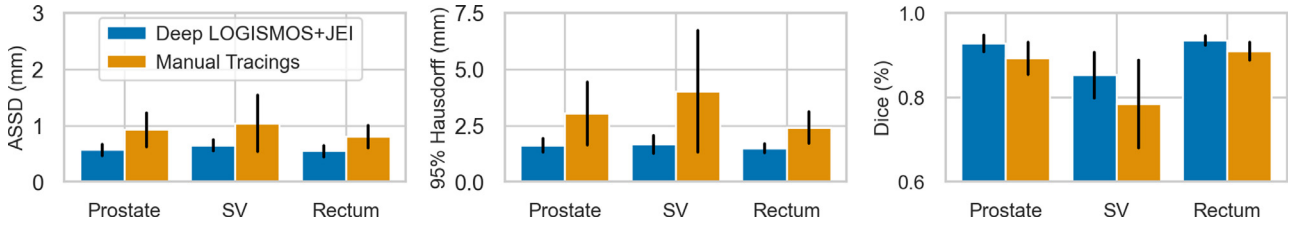

Figure 4 Performance and variability of Deep LOGISMOS + JEI compared with that of manual tracings by 3 expert radiation oncologists on 3 patients with a wide range of body mass index (21-32). ASSD, 95% Hausdorff distance, and Dice similarity coefficient are summarized (mean ± standard deviation). The error bars show variability of each approach. *Abbreviations:* ASSD = absolute surface-to-surface distances; JEI = just enough interaction; LOGISMOS = layered optimal graph image segmentation of multiple objects and surfaces; SV = seminal vesicles.

consensus STAPLE contours had a mean ASSD of 0.93, 1.04, and 0.81 mm for the prostate, seminal vesicles, and rectum, respectively. In comparison, the deviation of Deep LOGISMOS + JEI from consensus STAPLE contours was 0.57, 0.64, and 0.55 mm for the same organs.

Discussion

The results presented in this work are quite encouraging for improving the efficiency of adaptive therapy while still allowing clinician input and the ability to edit the contours more efficiently. One of the key advantages of our approach, afforded by the use of LOGISMOS after the initial deep learning presegmentation, is the fact that a limited data set (115 MR data sets in this case) can be used for training with excellent results. Our results indicate an excellent accuracy (median ASSD of <1 mm) with respect to expert contours. The relatively small training data set is an advantage for future implementations as new imaging sequences are expected to be employed. With regards to clinical implementation, we expect the fully automated functionality of Deep LOGISMOS will be used most often for radiation treatment planning, with the available JEI guidance used in situations of anatomic ambiguities or low image quality that consequently require specialized insights of a human expert. This is especially powerful as any automated segmentation method may fail in certain cases, but the use of JEI allows corrections to be made efficiently in 3D rather than in a slice-by-slice fashion.

Algorithms such as Deep LOGISMOS + JEI are expected to reduce one of the main operational challenges of MRIgART, which is the extended treatment session times compared with conventional cone beam computed tomography–based image guidance on traditional linear accelerators.[2,23] Contouring continues to be a time-consuming manual process, which is a major contributor to the treatment time and reduced patient throughput on MR linear accelerators. This work presents a more efficient and less user-intensive workflow which will increase throughput and may aid in accelerating the adoption of MRIgART in the broader radiation therapy community.[24] Furthermore, shorter treatment session times improve patient comfort and can reduce the magnitude of intrafraction motion which is an important factor in MRIgART, particularly when considering planned target volume margin reduction.[25-27] The rapid and accurate contouring presented in this work is expected to also be a valuable addition for future adaptive intrafraction planning.

It is important to note that efficiency is not the only advantage of the Deep LOGISMOS + JEI approach, as manual segmentation, even on high-quality MR images, is inherently nonreproducible. Nearly all the discrepancies between the manual and LOGISMOS + JEI results can be attributed to a lack of slice-to-slice consistency in the manually derived contours. It is expected that the improvements in contour reproducibility enabled by the Deep LOGISMOS + JEI approach will enable greater contouring standardization in radiation therapy. Additionally, accurate and reproducible organ/object segmentations in radiation therapy would translate into more reliable organ-specific functional imaging metrics for response assessment during radiation therapy, the repeatability of which has been previously investigated.[28,29] This opens the door for future application of radiomic analyses derived from these now readily available image contours.

Conclusion

This work demonstrates the potential of the Deep LOGISMOS + JEI approach to assist in the contouring of key structures in the ART workflow for the treatment of prostate cancer. Through accurate segmentation of key structures, this approach can limit the need for manual recontouring that can lead to decreased treatment times. Additionally, the autosegmentation with minor physician intervention could result in more consistent contours between fractions for a single patient as well as across multiple patients.

Disclosures

Daniel E. Hyer reports a relationship with Elekta that includes consulting or advisory, funding grants, and speaking and lecture fees. Joseph Caster reports a relationship with Elekta that includes funding grants. Joel St-Aubin reports a relationship with Elekta that includes funding grants and speaking and lecture fees. Jeffrey Snyder reports a relationship with Elekta that includes funding grants and speaking and lecture fees. Honghai Zhang reports financial support was provided by the National Institute of Biomedical Imaging and Bioengineering. Sean Mullan reports financial support provided by National Heart Lung and Blood Institute. John Buatti reports a relationship with American Society for Radiation Oncology that includes board membership. Milan Sonka reports financial support from the National Institute of Biomedical Imaging and Bioengineering.

References

1. Dunkerley D, Yaddanapudi S, Snyder J, Hyer D, St-Aubin J. Analysis of patient treatment time for adaptive work flows on the Elekta Unity. *Med Phys*. 2020;47:e578.
2. Paulson ES, Ahunbay E, Chen X, et al. 4D-MRI driven MR-guided online adaptive radiotherapy for abdominal stereotactic body radiation therapy on a high field MR-Linac: Implementation and initial clinical experience. *Clin Transl Radiat Oncol*. 2020;23:72-79.
3. Henke L, Kashani R, Robinson C, et al. Phase I trial of stereotactic MR-guided online adaptive radiation therapy (SMART) for the treatment of oligometastatic or unresectable primary malignancies of the abdomen. *Radiother Oncol*. 2018;126:519-526.
4. de Muinck Keizer DM, Kerkmeijer LGW, Willigenburg T, et al. Prostate intrafraction motion during the preparation and delivery of MR-guided radiotherapy sessions on a 1.5T MR-Linac. *Radiother Oncol*. 2020;151:88-94.
5. Lamb J, Cao M, Kishan A, et al. Online adaptive radiation therapy: Implementation of a new process of care. *Cureus*. 2017;9:e1618.
6. Delpon G, Escande A, Ruef T, et al. Comparison of automated atlas-based segmentation software for postoperative prostate cancer radiotherapy. *Front Oncol*. 2016;6:178.
7. Simmat I, Georg P, Georg D, Birkfellner W, Goldner G, Stock M. Assessment of accuracy and efficiency of atlas-based autosegmentation for prostate radiotherapy in a variety of clinical conditions. *Strahlenther Onkol*. 2012;188:807-815.
8. Zabel WJ, Conway JL, Gladwish A, et al. Clinical evaluation of deep learning and atlas-based auto-contouring of bladder and rectum for prostate radiation therapy. *Pract Radiat Oncol*. 2021;11:e80-e89.
9. Zhang L, Guo Z, Zhang H, et al. Assisted annotation in Deep LOGISMOS: Combining deep learning and graph optimization for simultaneous multi-compartment 3D segmentation of calf muscles on MRI. Available at: https://shorturl.at/ciJKO.
10. Yin Y, Fotin S, Periaswamy S, et al. Fully automated 3D prostate central gland segmentation in MR images: A LOGISMOS based approach. *Proc SPIE*. 2012;8314.
11. Zhang H, Lee K, Chen Z, Kashyap S, Sonka MLOGISMOS-JEI. Segmentation using optimal graph search and just-enough interaction. In: Zhou SK, Rueckert D, Fichtinger G, eds. *Handbook of Medical Image Computing and Computer Assisted Intervention*. San Diego, CA: Academic Press; 2020:249-272.
12. Li K, Wu X, Chen DZ, Sonka M. Optimal surface segmentation in volumetric images—A graph-theoretic approach. *IEEE Trans Pattern Anal Mach Intell*. 2006;28:119-134.
13. Yin Y, Zhang X, Williams R, Wu X, Anderson DD, Sonka M. LOGISMOS—Layered optimal graph image segmentation of multiple objects and surfaces: Cartilage segmentation in the knee joint. *IEEE Trans Med Imaging*. 2010;29:2023-2037.
14. Wu X, Dou X, Wahle A, Sonka M. Region detection by minimizing intraclass variance with geometric constraints, global optimality, and efficient approximation. *IEEE Trans Med Imaging*. 2011;30:814-827.
15. Sun S, Sonka M, Beichel RR. Graph-based IVUS segmentation with efficient computer-aided refinement. *IEEE Trans Med Imaging*. 2013;32:1536-1549.
16. Olszewski M, Wahle A, Vigmostad S, Sonka M. Multidimensional segmentation of coronary intravascular ultrasound images using knowledge-based methods. *Proc SPIE*. 2005:5747.
17. Haeker M, Wu X, Abramoff M, Kardon R, Sonka M. Incorporation of regional information in optimal 3-D graph search with application for intraretinal layer segmentation of optical coherence tomography images. *Inf Process Med Imaging*. 2007;20:607-618.
18. Garvin MK, Abramoff MD, Wu X, Russell SR, Burns TL, Sonka M. Automated 3-D intraretinal layer segmentation of macular spectral-domain optical coherence tomography images. *IEEE Trans Med Imaging*. 2009;28:1436-1447.
19. Oguz I, Sonka M. LOGISMOS-B: Layered optimal graph image segmentation of multiple objects and surfaces for the brain. *IEEE Trans Med Imaging*. 2014;33:1220-1235.
20. Xie Y, Zhang J, Shen C, Xia Y. CoTr: Efficiently bridging CNN and transformer for 3D medical image segmentation. Available at: https://ui.adsabs.harvard.edu/abs/2021arXiv210303024X. Accessed March 1, 2021.
21. Isensee F, Jaeger PF, Kohl SAA, Petersen J, Maier-Hein KH. nnU-Net: A self-configuring method for deep learning-based biomedical image segmentation. *Nature Methods*. 2021;18:203-211.
22. Warfield SK, Zou KH, Wells WM. Simultaneous truth and performance level estimation (STAPLE): An algorithm for the validation of image segmentation. *IEEE Trans Med Imaging*. 2004;23:903-921.
23. Snyder JE, St-Aubin J, Yaddanapudi S, et al. Reducing MRI-guided radiotherapy planning and delivery times via efficient leaf sequencing and segment shape optimization algorithms. *Phys Med Biol*. 2022;67: 055005.
24. Hehakaya C, Sharma AM, van der Voort Van Zijp JRN, et al. Implementation of magnetic resonance imaging-guided radiation therapy in routine Care: Opportunities and challenges in the United States. *Adv Radiat Oncol*. 2022;7: 100953.
25. Xie Y, Djajaputra D, King CR, Hossain S, Ma L, Xing L. Intrafractional motion of the prostate during hypofractionated radiotherapy. *Int J Radiat Oncol Biol Phys*. 2008;72:236-246.
26. de Muinck Keizer DM, van der Voort van Zyp JRN, de Groot-van Breugel EN, Raaymakers BW, Lagendijk JJW, de Boer HCJ. On-line daily plan optimization combined with a virtual couch shift procedure to address intrafraction motion in prostate magnetic resonance guided radiotherapy. *Phys Imaging Radiat Oncol*. 2021;19:90-95.
27. Willigenburg T, Zachiu C, Bol GH, et al. Clinical application of a subfractionation workflow for intrafraction re-planning during prostate radiotherapy treatment on a 1.5 Tesla MR-Linac: A practical method to mitigate intrafraction motion. *Radiother Oncol*. 2022;176:25-30.
28. Fedorov A, Vangel MG, Tempany CM, Fennessy FM. Multiparametric magnetic resonance imaging of the prostate: Repeatability of volume and apparent diffusion coefficient quantification. *Invest Radiol*. 2017;52:538-546.
29. Peled S, Vangel M, Kikinis R, Tempany CM, Fennessy FM, Fedorov A. Selection of fitting model and arterial input function for repeatability in dynamic contrast-enhanced prostate MRI. *Acad Radiol*. 2019;26:e241-e251.